PHYSICAL REVIEW A **74**, 031601(R) (2006)

Bose-Einstein-condensate interferometer with macroscopic arm separation

O. Garcia, B. Deissler, K. J. Hughes, J. M. Reeves, and C. A. Sackett*
Physics Department, University of Virginia, Charlottesville, Virginia 22904, USA
(Received 20 March 2006; published 11 September 2006)

A Michelson interferometer using Bose-Einstein condensates is demonstrated with coherence times of up to 44 ms and arm separations up to 180 μm. This arm separation is larger than that observed for any previous atom interferometer. The device uses atoms weakly confined in a magnetic guide and the atomic motion is controlled using Bragg interactions with an off-resonant standing-wave laser beam.

DOI: 10.1103/PhysRevA.74.031601 PACS number(s): 03.75.Dg, 39.20.+q

Atom interferometry, the matter-wave analog of light interferometry, works by splitting an atomic wave function into two packets that are separated in space [1,2]. When they are later recombined, the outcome depends on the difference in their quantum phases. Atom interferometry is a powerful measurement tool, because the phases depend strongly on effects such as inertial forces and electromagnetic fields. One limitation, however, has been the difficulty of splitting an ensemble of atoms into spatially distinct "arms." Although individual atomic wave functions can be split over distances of up to 1.1 mm [3,4], the atoms are typically located randomly within a cloud or beam that is several mm across. The separate packets are therefore not individually accessible in the way that the arms of an ordinary light interferometer are.

Some applications, such as gravity and rotation measurement, do not require distinct arms, and conventional atom interferometry has proven to be highly effective in these cases [3–6]. However, separated arms permit many additional uses. In a few atomic beam experiments, separated arms have been achieved by using tightly collimated beams and material diffraction gratings. This has enabled precise measurements of electric polarizability [7,8], phase shifts in atomic and molecular scattering [9], and atom-surface interactions [10]. A larger separation can be expected to have even more utility.

Atoms in a Bose-Einstein condensate are promising for interferometry due to their low velocities and high spatial coherence [11,12]. In this case, all the atoms share the same quantum state so the arm spacing is the same as the spacing of the individual atomic wave packets. Condensate interferometers with packet displacements of over 100 μm have been demonstrated [13,14], but the packets were even larger and did not separate. Distinct packets have been obtained by splitting a condensate between two optical traps [15,16], but the maximum spacing was only 13 μm, comparable to that achieved with beam interferometers. Recently, a similar spatial separation was obtained in a magnetic trap [17].

In our device, ^{87}Rb condensates are confined in a magnetic waveguide, as described in Ref. [18]. Condensates with roughly 10^4 atoms are produced and loaded into the guide, which is generated by a set of copper rods mounted in the vacuum chamber. The guide axis is horizontal and the atoms are held about 7 mm from the rod surfaces. Ideally, the guide would provide harmonic confinement only in the transverse directions, but the finite length of our rods leads to axial confinement as well. For the data presented here, the transverse oscillation frequencies are 3.3 Hz and 6 Hz, and the axial frequency is 1.2 Hz. This confinement is weaker than that of typical magnetic traps, offering some advantages discussed later.

The operation of the interferometer is illustrated in Fig. 1. The atoms are manipulated by Bragg scattering from an off-resonant standing-wave laser beam [19–21], with pulses of this beam splitting, reflecting, and then recombining the condensate as in Ref. [14]. During the splitting pulse, the beam couples atoms at rest in state $|0\rangle$ to two states $|\pm v_0\rangle$ moving with speed $v_0 \equiv 2\hbar k/M = 1.2$ cm/s, where $k \approx 2\pi/(780\ \text{nm})$ is the wave vector of the light and M the mass of the atoms. The coupling is induced by the ac Stark shift, which provides a potential energy $U = 2\hbar\beta \sin^2(kz-\alpha)$ with β proportional to the light intensity and α denoting the phase of the standing-wave pattern. Up to an unimportant constant, this can be simplified to

$$U = \frac{\hbar\beta}{2}(e^{-2i\alpha}e^{2ikz} + e^{2i\alpha}e^{-2ikz}), \tag{1}$$

from which it can be seen that the coupling amplitudes are proportional to $e^{\pm 2i\alpha}$. For the splitting pulse we take $\alpha = 0$ so that

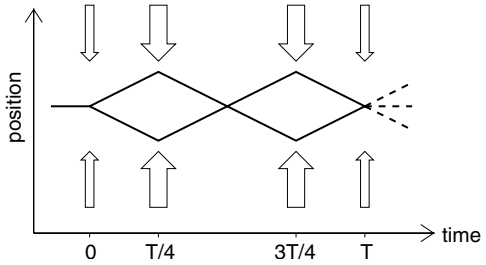

FIG. 1. Trajectory of wave packets in the interferometer. The condensate atoms begin nominally at rest. At $t=0$, an off-resonant laser beam (indicated by the arrows) splits the condensate into two packets traveling at ±1.2 cm/s. At times $T/4$ and $3T/4$, the laser is used to used to reverse the atoms' motion. At time T, a recombining pulse brings the atoms back to rest with a probability that depends on the interferometer phase. The moving atoms (if any) continue to propagate until the system is imaged to determine the output state.

*Electronic address: sackett@virginia.edu

$$|0\rangle \rightarrow |+\rangle \equiv \frac{1}{\sqrt{2}}(|+v_0\rangle + |-v_0\rangle). \quad (2)$$

After the splitting pulse, the packets freely propagate until $t=T/4$, when the Bragg beam is applied so as to reverse the packets' direction of motion. The packets then propagate for time $T/2$, crossing each other and separating on the other side. They are reflected again at $t=3T/4$ and return to their initial position at time T. If the packets acquire a differential phase ϕ during their propagation, their state is now

$$|\phi\rangle = \frac{1}{\sqrt{2}}(e^{i\phi/2}|+v_0\rangle + e^{-i\phi/2}|-v_0\rangle). \quad (3)$$

Since the packets make a full oscillation in the guide, any phase shift resulting from asymmetry in the potential cancels to first order, and ϕ is nominally zero. We used this geometry so that the interferometer could be tested with no uncontrolled phase effects.

The packets are recombined by applying the same Bragg pulse used for splitting, but with a variable standing-wave phase α. The pulse therefore couples $|0\rangle$ to the state

$$|\alpha\rangle = \frac{1}{\sqrt{2}}(e^{2i\alpha}|+v_0\rangle + e^{-2i\alpha}|-v_0\rangle). \quad (4)$$

The probability for the recombination pulse to return an atom to rest at the end of the experiment is given by the overlap between $|\phi\rangle$ and $|\alpha\rangle$, or $|\langle\alpha|\phi\rangle|^2=\cos^2(\phi/2-2\alpha)$. After the recombination pulse, the packets are allowed to separate for 40 ms and the atoms are then imaged. The fraction of atoms in the packet at rest is the output signal of the device.

The Bragg beam is derived from a diode laser detuned about 8.4 GHz red of the $5S_{1/2}$ to $5P_{3/2}$ laser cooling transition. For the splitting and combining operations, we obtain good results using a double-pulse sequence with the theoretically optimum values of $2^{-5/2}\pi/\omega_r=24$ μs for the pulse duration and $\pi/(4\omega_r)=33$ μs for the delay between pulses [22]. Here $\omega_r=\hbar k^2/(2M)$ is the recoil frequency. The beam power is 0.7 mW with a Gaussian beam waist of approximately 1.5 mm.

The reflection pulse can be implemented using second-order Bragg coupling between the $|+v_0\rangle$ and $|-v_0\rangle$ states [20]. However, this method is very sensitive to velocity errors. Our condensates sometimes start with a nonzero velocity, because external magnetic fields can easily disturb the process of loading the atoms into the waveguide. We observed this motion by taking two pictures of the same cloud using phase contrast imaging. The residual velocity appears to vary randomly, with a magnitude of up to 0.5 mm/s. In the interferometer, an atom moving with velocity $v_0+\delta$ will be reflected to velocity $-v_0+\delta$, yielding an energy difference $\Delta E=2Mv_0\delta$. If the reflection pulse has duration τ_r, then ΔE must be small compared to $\hbar/\tau_r$ for the transition to occur. This requires $|\delta| \lesssim \hbar/(2Mv_0\tau_r)$. For instance, Wang *et al.* [14] used $\tau_r=150$ μs, requiring $|\delta| \lesssim 0.2$ mm/s, which is violated in our experiment.

Increasing the Bragg laser intensity decreases τ_r, but also induces coupling to the off-resonant $|0\rangle$ state. We developed a technique that makes use of this coupling. For $\alpha=0$, the Bragg beam couples the $|0\rangle$ and $|+\rangle$ states, making an effective two-level system. The orthogonal state $|-\rangle=(|+v_0\rangle-|-v_0\rangle)/\sqrt{2}$ is not coupled, but does acquire a phase shift while the light is on. We choose the pulse intensity and duration so that the atoms make two full Rabi oscillations between the $|+\rangle$ and $|0\rangle$ states, ultimately leaving their state unchanged. During this evolution, atoms in the $|-\rangle$ state acquire a phase of π. This causes $|+v_0\rangle=(|+\rangle+|-\rangle)/\sqrt{2}$ to evolve to $(|+\rangle-|-\rangle)/\sqrt{2}=|-v_0\rangle$ and vice versa, achieving the desired reflection. The nominal pulse duration is $\pi/(2\omega_r)\approx 67$ μs and the amplitude is $\beta=\sqrt{24}\omega_r$, corresponding to an intensity $\sqrt{3}$ times higher than that of the splitting pulse. The shorter pulse duration makes this method less sensitive to the packet velocity, requiring $|\delta| \lesssim 0.5$ mm which we marginally satisfy. We observe this pulse to work fairly well, with reflection efficiencies varying between about 80% and 100%. This variation can presumably be attributed to the fluctuations in atomic velocity.

To observe the operation of the interferometer, we vary the recombination phase α. The Bragg standing wave is generated using a mirror outside the vacuum chamber, located a distance $D=22.5$ cm from the atoms. When the laser frequency is changed by Δf, the standing-wave phase shifts by $\alpha=(2\pi D/c)\Delta f$. The frequency change is accomplished in 2 ms by adjusting the current of the diode laser.

Figure 2 shows the results of the interference experiment. Figure 2(a) shows example images of the spatial distribution of the atoms for various α. Figure 2(b) plots the fraction of atoms brought to rest and exhibits the interference fringe. We performed similar experiments for various values of the packet propagation time T, finding the visibility of the interference to vary as indicated in Fig. 2(c). Interference is observed for T as large as 44 ms. Most previous experiments with condensates have been limited to a coherence time of 10 ms or less [14], although a result of 200 ms has been recently reported [17].

We attribute the long coherence time of our experiment to the weak confinement of our guide. In particular, atomic interactions are much weaker due to the lower density. As noted by Olshanii and Dunjko [23], interactions induce a phase gradient on the packets as they separate, since one end of a packet stops interacting with the opposing packet immediately while the other end must traverse the entire condensate length. If it takes time τ for the two packets to fully separate, the differential phase is on the order of $\mu\tau/\hbar$ for chemical potential μ. This can spoil the interference effect as different parts of the condensate will recombine with different phases. Using the Thomas-Fermi approximation [24], the chemical potential of our initial condensate is $\mu \approx 2\pi\hbar \times 10$ Hz, yielding a phase of about 0.2 rad for $\tau=3$ ms. In comparison, the experiment of Wang *et al.* [14] had a separation phase of about 3.3 rad. Weak confinement also reduces the sensitivity to vibrations of the trap structure and requires less precise alignment of the Bragg beam to the guide axis [22].

As seen in Fig. 2, we do not observe perfect interference even for small T. This is due to run-to-run fluctuations in the interferometer output that lower the average visibility. This variation could be attributed to the Bragg beam, but we

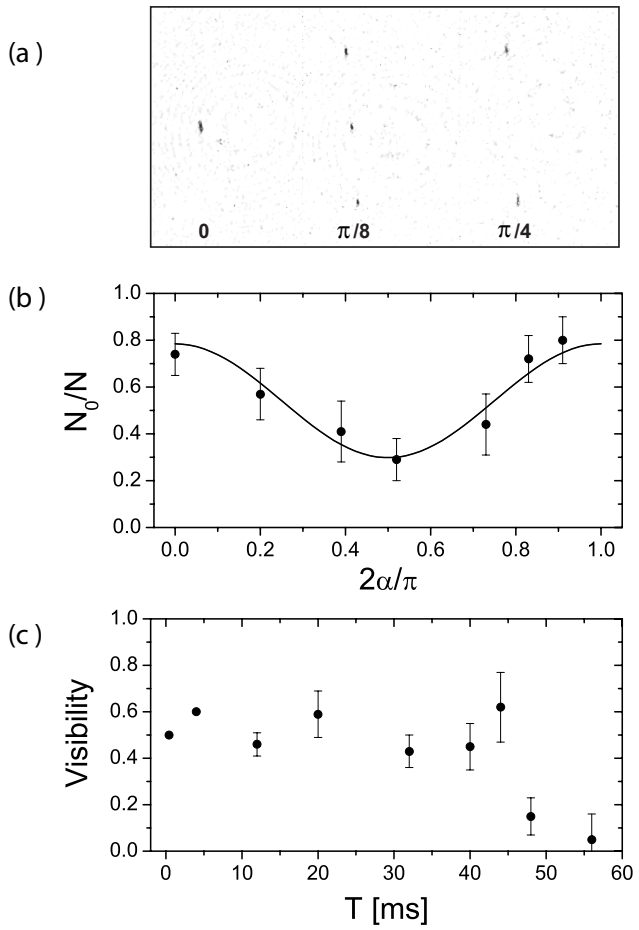

FIG. 2. Interferometer results. (a) Absorption images of the interferometer output for the indicated standing wave phases α. The dark spots show the positions of the three output wave packets. These images are analyzed by fitting each peak to a Gaussian function to estimate the fraction of atoms at rest, N_0/N. Imaging noise introduces errors of about ±0.05 to this ratio. (b) Interference fringe for $T=40$ ms. For each value of the standing-wave phase α, several images were taken and the average value of N_0/N was determined. The error bars show the standard deviation of the mean. The solid curve is a fit to the function $y_0+A\cos(4\alpha)$ yielding amplitude $A=0.24\pm0.05$ and offset $y_0=0.54\pm0.04$. The visibility V is calculated as $A/y_0=0.45\pm0.10$. (c) Visibility as a function of interaction time. For times $T>10$ ms, a set of data such as (b) was acquired and fit to determine the visibility V. For the shorter times, it was not possible to change the laser wavelength quickly enough, so a set of points at $\alpha=0$ only were used to estimate the visibility as $V\approx 2\langle N_0/N\rangle-1$.

monitor the stability of the laser and mirror using an optical interferometer and observe no significant noise. The Bragg beam does, however, contain spatial noise that modulates the beam intensity by about 20%. Pointing fluctuations in the beam therefore change the Bragg coupling strength and causes the splitting and reflection operations to vary, introducing errors into the interferometer output. Another source of noise is the residual condensate motion mentioned previously, which degrades the performance of the reflection pulses.

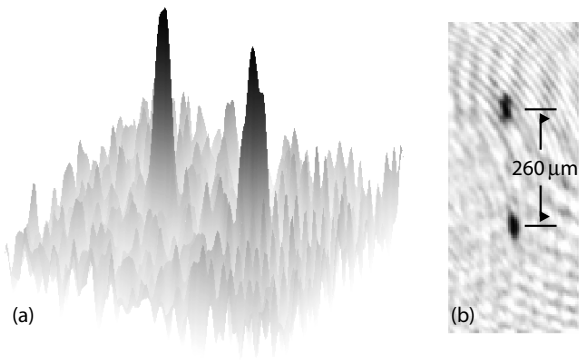

FIG. 3. Separated packets in the interferometer, here shown as both a three-dimensional image (a) and a flat picture (b). The absorption image was taken 11 ms after the splitting pulse and illustrates the maximum separation for an experiment with $T=44$ ms. Since the interference visibility is nonzero for this T, the atoms in this picture are in a quantum superposition of being in both peaks. The center-to-center separation of the two peaks is 0.26 mm.

At longer times, the run-to-run fluctuations increase until the visibility drops to zero. The drop appears abrupt, though the error bars are also consistent with a more gradual decline. Various noise sources might cause this, but it might also stem from the condensate motion. Another effect of the motion is to make the splitting pulse asymmetric, producing more atoms in one packet than the other. Typical asymmetries are about 20%. The packet with more atoms has a larger self-interaction energy, leading to a phase shift that fluctuates with the velocity and increases with T. The observed decoherence time is reasonably consistent with this effect, but a detailed calculation is difficult because the packets evolve in a complex way over time.

For $T=44$ ms, the maximum center-to-center packet distance is $2v_0T/4=260$ μm. Figure 3 shows an image taken at this point. Each packet has a full width of about 80 μm, leaving a 180 μm spacing between the packets. To our knowledge, this is the first literal picture of a matter wave that has been split into two demonstrably coherent pieces, illustrating a fundamental principle of quantum mechanics in a concrete way and on a scale that is appreciable to the senses.

This large separation also offers the potential for novel applications. For instance, one arm of the interferometer might pass into a small optical cavity, acquiring a phase shift that depends on the cavity field. In this way the number of photons in the cavity could be measured in a nondestructive way, similar to the experiments of Nogues *et al.* [25]. In comparison, an interferometer would be sensitive to smaller phase shifts, allowing the atom-photon interaction to be nonresonant and making the technique simpler and more flexible. This could be useful for applications in quantum communication.

Another possibility would be to have one arm bounce off a material surface through quantum reflection [26,27]. This would allow measurement of the reflection phase shift and provide a sensitive probe of effects such as the Casimir-Polder force. Although both arms of our interferometer

traverse the same path, improvements in the waveguide field stability and homogeneity should allow operation with separate paths. Alternatively, the motion of the atoms is slow enough that the surface could be mechanically displaced before the second packet arrives.

In summary, we have demonstrated a condensate interferometer with wave packet separations of up to 0.26 mm and clear arm spacing of up to 0.18 mm. This is by a large margin the greatest arm spacing ever observed in an atom interferometer. To improve our results, we need to improve the quality of the splitting and reflecting operations. We hope to achieve this by using better chamber windows to permit a more uniform beam, and by better controlling the net magnetic field while loading the guide. If successful, we estimate that an additional order of magnitude improvement in packet separation should be possible before encountering limitations such as phase diffusion [28]. We hope that the techniques demonstrated here will help condensate interferometers realize their promise for novel measurement applications.

We are grateful to E. A. Cornell and R. R. Jones for useful discussions and to K. L. Baranowski and J. H. T. Burke for their work on the experiment. This work was sponsored by the Office of Naval Research (Grant No. N00014-02-1-0454) and the National Science Foundation (Grant No. PHY-0244871).

[1] *Atom Interferometry*, edited by P. R. Berman (Academic Press, San Diego, 1997).
[2] D. E. Pritchard, A. D. Cronin, S. Gupta, and D. A. Kokorowski, Ann. Phys. **10**, 35 (2001).
[3] A. Peters, K. Y. Chung, and S. Chu, Metrologia **38**, 25 (2001).
[4] J. McGuirk, G. Foster, J. Fixler, M. Snadden, and M. Kasevich, Phys. Rev. A **65**, 033608 (2002).
[5] T. L. Gustavson, A. Landragin, and M. A. Kasevich, Class. Quantum Grav. **17**, 2385 (2000).
[6] A. Wicht, E. Hensley, J. M. Sarajlic, and S. Chu, Phys. Scr., T **102**, 82 (2002).
[7] C. R. Ekstrom, J. Schmiedmayer, M. S. Chapman, T. D. Hammond, and D. E. Pritchard, Phys. Rev. A **51**, 3883 (1995).
[8] A. Miffre, M. Jacquey, M. Büchner, G. Trénec, and J. Vigué, Phys. Rev. A **73**, 011603(R) (2006).
[9] J. Schmiedmayer, M. S. Chapman, C. R. Ekstrom, T. D. Hammond, S. Wehinger, and D. E. Pritchard, Phys. Rev. Lett. **74**, 1043 (1995).
[10] J. D. Perreault and A. D. Cronin, Phys. Rev. Lett. **95**, 133201 (2005).
[11] K. Bongs and K. Sengstock, Rep. Prog. Phys. **67**, 907 (2004).
[12] J. Dunningham, K. Burnett, and W. D. Phillips, Philos. Trans. R. Soc. London, Ser. A **363**, 2165 (2005).
[13] S. Gupta, K. Dieckmann, Z. Hadzibabic, and D. E. Pritchard, Phys. Rev. Lett. **89**, 140401 (2002).
[14] Y. J. Wang, D. Z. Anderson, V. M. Bright, E. A. Cornell, Q. Diot, T. Kishimoto, M. Prentiss, R. A. Saravanan, S. R. Segal, and S. Wu, Phys. Rev. Lett. **94**, 090405 (2005).
[15] Y. Shin, M. Saba, T. A. Pasquini, W. Ketterle, D. E. Pritchard, and A. E. Leanhardt, Phys. Rev. Lett. **92**, 050405 (2004).
[16] M. Saba, T. A. Pasquini, C. Sanner, Y. Shin, W. Ketterle, and D. E. Pritchard, Science **307**, 1945 (2005).
[17] G-B. Jo, Y. Shin, S. Will, T. A. Pasquini, M. Saba, W. Ketterle, D. E. Pritchard, M. Vengalattore, and M. Prentiss, e-print cond-mat/0608585.
[18] J. M. Reeves, O. Garcia, B. Deissler, K. L. Baranowski, K. J. Hughes, and C. A. Sackett, Phys. Rev. A **72**, 051605(R) (2005).
[19] P. J. Martin, B. G. Oldaker, A. H. Miklich, and D. E. Pritchard, Phys. Rev. Lett. **60**, 515 (1988).
[20] D. M. Giltner, R. W. McGowan, and S. A. Lee, Phys. Rev. A **52**, 3966 (1995).
[21] M. Kozuma, L. Deng, E. W. Hagley, J. Wen, R. Lutwak, K. Helmerson, S. L. Rolston, and W. D. Phillips, Phys. Rev. Lett. **82**, 871 (1999).
[22] S. Wu, E. J. Su, and M. Prentiss, Eur. Phys. J. D **35**, 111 (2005).
[23] M. Olshanii and V. Dunjko, e-print cond-mat/0505358.
[24] F. Dalfovo, S. Giorgini, L. Pitaevskii, and S. Stringari, Rev. Mod. Phys. **71**, 463 (1999).
[25] G. Nogues, A. Rauschenbeutel, S. Osnaghi, M. Brune, J. M. Raimond, and S. Haroche, Nature (London) **400**, 239 (1999).
[26] F. Shimizu, Phys. Rev. Lett. **86**, 987 (2001).
[27] T. A. Pasquini, Y. Shin, C. Sanner, M. Saba, A. Schirotzek, D. E. Pritchard, and W. Ketterle, Phys. Rev. Lett. **93**, 223201 (2004).
[28] J. Javanainen and M. Wilkens, Phys. Rev. Lett. **78**, 4675 (1997).